

OUTPUT SYNCHRONIZATION FOR TELEOPERATION OF WHEEL MOBILE ROBOT

Patrick Miller, Leng-Feng Lee, and Venkat Krovi

Mechanical and Aerospace Engineering
State University of New York at Buffalo
Buffalo, New York, USA
[pmiller4, llee3, vkrovi]@eng.buffalo.edu

ABSTRACT

The potential for use of robotic systems in remote applications arenas has long motivated development of robust and stable means of teleoperated control of slave systems. However, telerobotic systems face challenges stemming from the devices themselves, environmental factors, communication and control complexities. To address these challenges, we will adopt the passivity based synchronization framework [1] and study its applicability to safely synchronize two heterogeneous Lagrangian systems. Within this framework, an adaptive controller identifies and stabilizes the dynamics of the master and slave systems and renders the dynamics passive to a secondary coupling input. The passive mapping used to couple the output states of the master and slave systems and is made insensitive to lossy and delayed communication medium. Specifically, an adaptive passive synchronization teleoperation controller is developed between an Omni haptic device that serves as our master and a differentially driven nonholonomic Wheel Mobile Robot (WMR) as the slave system. A battery of hardware-in-the-loop simulations are used to verify the proposed controller.

1 INTRODUCTION

Teleoperation offers humans the ability to extend their own reach and senses over various length and timescales in innumerable applications. These applications include remote control of semi autonomous robotic system in hazardous and remote environment from minimally invasive surgeries to deep-sea and planetary exploration.

In a typical teleoperation setup, a user controls a master manipulator device that can range from a joystick to multi-degree of freedom force reflecting (haptic) device. The user's commands are transmitted through a communication medium to the slave device (a distant robotic manipulator), which attempts to execute received commands while interacting within the remote environment. The experienced forces and motions from the slave device-environmental interactions are communicated (and

reflected in a scaled manner) back to the user. The reflected force allows the user to control the slave with kinesthetic cues, which along with auditory or visual feedback, allows a sense of immersion (telepresence) in the distant environment.

Telerobotic systems are faced with many complex issues stemming from: (i) master/slave devices themselves, (ii) environmental factors, (iii) communication delays, and (iv) control complexities. First and foremost the master and slave systems are typically complex electromechanical systems individually - requiring kinematically and dynamically dissimilar systems to interact and work together which can be challenging even in idealized environments with perfect/lossless communication. Second, slave systems are often placed in highly unstructured and diverse environments, typically not understood a priori, and failure to account for environmental interaction or varying conditions could lead to destabilization. Significant challenges also arise from the communication limitations and imperfections. The diversity of network architecture, protocols and loads can result in limited, lossy and variable delay communication between the master and slave machines. Last, but not least, is the contribution and role of the human user. The requirement for transparency of force feedback requires high sampling rates (1000 Hz or higher). This sampling rate puts a significant burden on the control algorithm to be computationally efficient while retaining performance and accuracy. Model-based nonlinear controllers with adaptivity can provide improved results, but depend significantly on accurate models and can increase computational burden of the slave robot.

Over decades, researchers continue to devote an extensive amount of effort to understanding complexities of bilateral control over time delayed networks. Satisfying the competing/conflicting tradeoff between stability and transparency continues to pose challenges to teleoperation to this day. An extensive survey of bilateral teleoperation schemes was presented in [2]. Until recently, the wave-variable based framework introduced in [3] and [4] has been at the forefront of teleoperation research with

many variants ensuing thereafter [5-9]. Unfortunately, these controllers would suffer from position drift if an initial position error exists between master and slave since only velocity and force information is typically exchanged in between master and slave (exceptions to this rule are [6, 7], which directly address the problem of position drift).

The output synchronization framework for Lagrangian systems presented by Chopra, Spong and Lozano in [10] was intended to overcome some of these limitations. Passivity based controllers take advantage of the inherent (passive) structure of rigid body systems to achieve the desired behavior [10-12]. This framework was developed and theoretically proven to result in stable teleoperation between homogenous Lagrangian systems. This framework successfully incorporates adaptive nonlinear control, and drift-less stable teleoperation without the use of wave variables. In [1] the stability of this framework for use in teleoperation was proven through the extensive use of Lyapunov analysis.

We will adopt this framework and study its applicability to safely synchronize heterogeneous Lagrangian systems for teleoperation. on the specific contribution of this work came from adapting this teleoperation controller for use with an Omni haptic device as our master and a differentially driven nonholonomic WMR as the slave system. This was then systematically tested within a Hardware-in-the-loop (HIL) framework with a physical haptic master (Omni) and a simulated/virtual slave (WMR). We not that a non-adaptive bilateral teleoperation scheme for wheeled mobile robots was presented in [13]. In contrast, we demonstrate that the adaptivity allows for increased robustness despite model uncertainties and disturbances.

The remainder of this paper is organized in the following fashion: Section 2 develops a brief overview of the passivity based output synchronization framework. In Section 3, the synchronization framework is adapted for the wheeled mobile robot slave and the Phantom Omni master. Section 4 focuses on the hardware in the loop setup. Section 5 describes the test scenarios and discusses the simulation results. Finally, Section 6 contains a brief discussion and future work.

2 CONTROL DESIGN

We adopt the output synchronization framework for two generic Lagrangian systems, establish the link between output synchronization and robust passivity control. This is briefly outlined here and the reader is referred to [14] for details.

The synchronization control strategy aims at solving two goals. A local nonlinear feedback control law is employed to render the local dynamics passive with respect to a secondary control input and output containing both position and velocity information. The secondary input is the kinematic coupling between master and slave, which is passive in nature and insensitive to communication delay. This framework has been expanded to include a basic viscous friction term which will lower our required damping ratio during high delay operation.

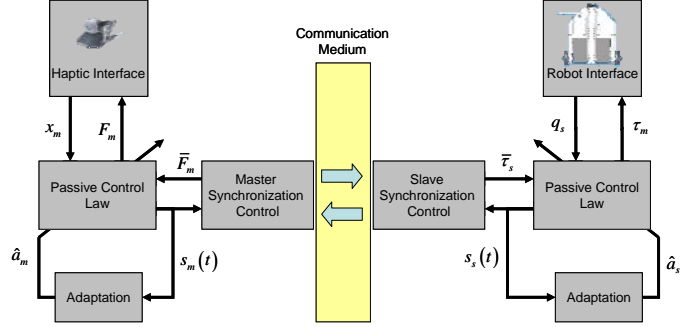


FIGURE 2. THE CONTROL SCHEME FLOWCHART

2.1 Robust Passivity Control of Individual System

We will begin with the standard representation of an n-link robotic manipulator:

$$\mathbf{M}(q)\ddot{q} + \mathbf{C}(q, \dot{q})\dot{q} + \mathbf{D}(q, \dot{q})\dot{q} = \tau \quad (1)$$

Our goal is to drive the manipulator end effector through a desired joint trajectory. The desired position, velocity and acceleration terms are denoted by q_d , \dot{q}_d , and \ddot{q}_d . The control law augments the existing state dynamics with the reference state vector \dot{q}_r given by:

$$\dot{q}_r = \dot{q}_d - \lambda \tilde{q} \quad \text{and} \quad \ddot{q}_r = \ddot{q}_d - \lambda \dot{\tilde{q}} \quad (2)$$

where, $\tilde{q} = q - q_d$, $\dot{\tilde{q}} = \dot{q} - \dot{q}_d$, and λ is a diagonal positive constant matrix. The manipulator control law is given by:

$$\tau = \hat{\mathbf{M}}(q)\ddot{q}_r + [\hat{\mathbf{C}}(q, \dot{q}) + \hat{\mathbf{D}}(q, \dot{q})]\dot{q}_r + u \quad (3)$$

where $\hat{(\cdot)}$ represents the estimated model parameter and u is a secondary control input. For Lagrangian system, the control law can be rewritten in a compact form:

$$\tau = \mathbf{Y}(\ddot{q}_r, \dot{q}_r, q)\hat{a} + u \quad (4)$$

yielding the closed-loop dynamical system as:

$$\mathbf{M}(q)\dot{s} + [\mathbf{C}(q, \dot{q}) + \mathbf{D}(q, \dot{q})]s = \mathbf{Y}(\ddot{q}_r, \dot{q}_r, q)\tilde{a} + u$$

where, $s = \dot{q} - \dot{q}_r = \dot{\tilde{q}} + \lambda \tilde{q}$, \tilde{a} is the estimated parameter error given by $\hat{a} - a$. The resulting closed loop equations can be rearranged into a state space form:

$$\dot{x} = \mathbf{f}(x) + \mathbf{g}(x)u, \quad x = [q \quad s]^T \quad (5)$$

where,

$$\mathbf{f}(x) = \begin{pmatrix} s + \dot{q}_r \\ \mathbf{M}(q)^{-1} \{ \mathbf{Y}(\ddot{q}_r, \dot{q}_r, q)\tilde{a} - [\mathbf{C}(q, \dot{q}) + \mathbf{D}(q, \dot{q})]s \} \end{pmatrix};$$

$$\mathbf{g}(x) = \begin{pmatrix} 0 \\ \mathbf{M}(q)^{-1} \end{pmatrix}$$

If the model parameters are perfectly known the above system is passive with respect to the control input u and output s using the storage function:

$$V(x) = s^T \mathbf{M}s \quad (6)$$

In the case of uncertain dynamic parameters, this passive property can be maintained by adding an adaptation law for the model parameters [11]:

$$u = -\mathbf{K}s + \ddot{u} \quad (7)$$

where \mathbf{K} is a constant positive diagonal matrix.

2.2 Passivity of Coupling Terms

Using the dynamic formulation above, the general dynamics for a master and slave system as can be expressed as:

$$\begin{aligned} \mathbf{M}_m(q)\ddot{q}_m + \mathbf{C}(q,\dot{q})_m\dot{q}_m + \mathbf{D}(\dot{q})_m\dot{q}_m &= \tau_m \\ \mathbf{M}_s(q)\ddot{q}_s + \mathbf{C}(q,\dot{q})_s\dot{q}_s + \mathbf{D}(\dot{q})_s\dot{q}_s &= \tau_s \end{aligned} \quad (8)$$

where the subscripts m and s represent the master and slave systems, respectively. The first step is to develop a local controller which renders the systems passive for a kinematic output. Using an estimated model, we apply the control:

$$\begin{aligned} \tau_m &= \hat{\mathbf{M}}(q)_m\ddot{q}_m^r + \hat{\mathbf{C}}(q,\dot{q})_m\dot{q}_m^r + \hat{\mathbf{D}}(\dot{q})_m\dot{q}_m^r + \bar{\tau}_m \\ \tau_s &= \hat{\mathbf{M}}(q)_s\ddot{q}_s^r + \hat{\mathbf{C}}(q,\dot{q})_s\dot{q}_s^r + \hat{\mathbf{D}}(\dot{q})_s\dot{q}_s^r + \bar{\tau}_s \end{aligned} \quad (9)$$

where τ_m and τ_s are the master and slave control inputs, $\langle \cdot \rangle$ represents the estimated model parameter, $\bar{\tau}_m$ and $\bar{\tau}_s$ are secondary controls used for synchronization and the new joint reference states are given by:

$$\dot{q}_i^r = -\lambda q_i \text{ and } \ddot{q}_i^r = -\lambda \dot{q}_i$$

where λ is a positive constant matrix. This control law represents the same robust passive control law outline in previous section, where the desired trajectory is the origin ($q_d = \dot{q}_d = \ddot{q}_d = 0$). The difference between the control laws is the addition of the secondary coupling control inputs. If the system dynamics are calculated using the method outlined about, the system dynamics can be written in a regressor form:

$$\begin{aligned} \tau_m &= \mathbf{Y}(q,\dot{q}_m^r,\ddot{q}_m^r)_m \hat{a}_m + \bar{\tau}_m \\ \tau_s &= \mathbf{Y}(q,\dot{q}_s^r,\ddot{q}_s^r)_s \hat{a}_s + \bar{\tau}_s \end{aligned} \quad (10)$$

Applying the control law yields the following closed loop system dynamics:

$$\begin{aligned} \dot{q}_m &= s_m - \lambda q_m \\ \mathbf{M}_m(q)\dot{s}_m + [\mathbf{C}(q,\dot{q})_m + \mathbf{D}(\dot{q})_m]s_m &= \mathbf{Y}(q_m,s_m)_m \tilde{a}_m + \bar{\tau}_m \\ \dot{q}_s &= s_s - \lambda q_s \\ \mathbf{M}_s(q)\dot{s}_s + [\mathbf{C}(q,\dot{q})_s + \mathbf{D}(\dot{q})_s]s_s &= \mathbf{Y}(q_s,s_s)_s \tilde{a}_s + \bar{\tau}_s \end{aligned} \quad (11)$$

where $s_i = \dot{q}_i + \lambda q_i \forall i \in m, s$. As in the robust passive control case, the parameter error prevents the closed loop systems from being

output passive. Hence, a parameter update law is introduced to maintain the passivity of the each local system:

$$\begin{aligned} \dot{\hat{a}}_m &= -\Gamma^{-1}\mathbf{Y}(q_m,s_m)_m^T s_m \\ \dot{q}_m &= -\lambda q_m + s_m \end{aligned} \quad (12)$$

$$\begin{aligned} \mathbf{M}_m(q)\dot{s}_m + [\mathbf{C}(q,\dot{q})_m + \mathbf{D}(\dot{q})_m]s_m &= \mathbf{Y}(q_m,s_m)_m \tilde{a}_m + \bar{\tau}_m \\ \dot{\hat{a}}_m &= -\Lambda^{-1}\mathbf{Y}(q_s,s_s)_s^T s_s \\ \dot{q}_s &= -\lambda q_s + s_s \end{aligned} \quad (13)$$

$$\mathbf{M}_s(q)\dot{s}_s + [\mathbf{C}(q,\dot{q})_s + \mathbf{D}(\dot{q})_s]s_s = \mathbf{Y}(q_s,s_s)_s \tilde{a}_s + \bar{\tau}_s$$

The above systems are now passive with respect to the secondary control input $\bar{\tau}_i$ and output s_i (for $i = m, s$).

2.3 Parameter Adaptation

The parameter update law for the adaptive synchronization law is the product of two time varying parameters.

$$\mathbf{Y}(q_i,s_i)_i^T s(t), \text{ where } i = m, s$$

As pointed out in [15], despite being bounded, these two vectors, are not guaranteed to stop being updated once steady state had been reached. From the control law, it is obvious that the estimated parameters affect the transient performance of the coupled systems. Therefore a gradient projection method is implemented to restrict the estimates of \hat{a}_i to inside a bounded convex set as suggested in [15]. The gradient projection method developed in [16] is given by:

$$\hat{a}_i = \begin{cases} \Gamma^{-1}\mathbf{Y}_i^T s_i & \text{if } \hat{a}_i^T \hat{a}_i < M_0^2 \text{ or} \\ \Gamma^{-1}\mathbf{Y}_i^T s_i & \text{if } \hat{a}_i^T \hat{a}_i = M_0^2 \text{ and } (\Gamma^{-1}\mathbf{Y}_i^T s_i)^T \hat{a}_i \leq 0 \\ \left(\mathbf{I} - \frac{\Gamma^{-1}\hat{a}_i\hat{a}_i^T}{\hat{a}_i^T \Gamma^{-1}\hat{a}_i} \right) \Gamma^{-1}\mathbf{Y}_i^T s_i & \text{otherwise} \end{cases} \quad (14)$$

where $\hat{a}(0)_i$ is chosen so $\hat{a}(0)_i^T \hat{a}(0)_i \leq M_0^2$ and $\mathbf{Y}_i = \frac{s_i}{m^2}$ where m^2 the normalizing constant $\dot{q}_r^T \dot{q}_r$, $\Gamma = \Gamma^T > 0$.

2.4 Hybrid Teleoperation Control

It is ideal to have the ability to reposition the master device before activating the kinematic coupling control law when implementing a synchronization control law. A hybrid controller, which can turn on and off the coupling control between master and slave, was implemented. The hybrid system has two states; a coupling state and holding state which is triggered by a flag (H_{on}). When $H_{on} \geq 1$, the controller is in the coupling state and the master and slave are synchronized using the control law outlined in previous section. When $H_{on} < 1$ the force feedback on the master system is turned off and the slave system follows the new secondary control:

$$\begin{aligned} \bar{\tau}_s &= -\mathbf{K}s_s(t) \\ \dot{q}_r &= -\lambda(q - q_c) \end{aligned} \quad (15)$$

where q_c is the actual joint state of the slave manipulator at the time H_{on} is switched off ($H_{on} < 1$). The new secondary control law is fed into the primary controller outlined above:

$$\tau_s = -\mathbf{Y}(q, \dot{q})_s \hat{a}_s + \bar{\tau}_s \quad (16)$$

The resulting control is identical to the robust passivity control law discussed in section 3 that drives to the slave system to exponentially converge to the q_c joint state until the coupling control is turned on. The passivity controller will be turned off for the master system leaving it free to move under the users' influence. This gives the user the ability to reposition the master system before reengaging the kinematic coupling control law.

3 SYNCHRONIZATION CONTROL OF A WMR

A Cartesian based synchronization control law is introduced for teleoperation of a WMR. Dynamic systems containing both holonomic and nonholonomic constraints, like the WMR, are not input-state linearizable by static state feedback [17]. However, given the proper set of output equations, this type of system may be input-output linearizable [18] which we adopt. To create an input-output mapping a decoupling matrix for the WMR must first be developed. When using this framework, care should be taken to assess and analyze the stability of any zero dynamics are presented in [19].

3.1 Dynamics of Wheeled Mobile Robot

The wheeled robot is a differentially driven base with two collinear drive wheels with motors attached. A base frame, $\{B\}$ is attached to the center of mass of the mobile base and is located at point (x_b, y_b) with respect to the inertial frame, $\{O\}$. A coordinate frame is also attached on the left and right wheels with the axis of rotation collinear to the body fixed y axis. A look ahead point (and coordinate frame) is arbitrarily defined a distance L_a from the body fixed frame along the body fixed x axis. It is assumed the center of mass, wheel frames and look ahead frames are all coplanar with the x-y plane.

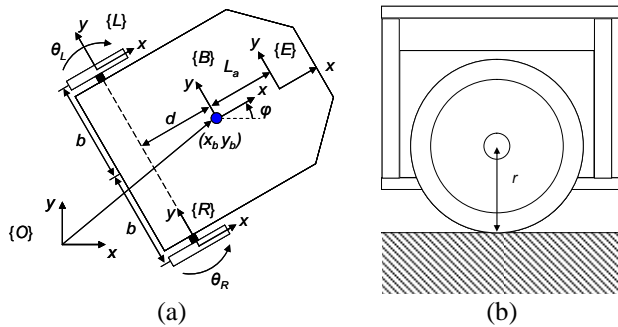


FIGURE 1. THE WMR SYSTEM A) TOP AND B) SIDE VIEW

The actuation and joint spaces are $\tau = [\tau_R \ \tau_L]^T$ and $\theta = [\theta_R \ \theta_L]^T$, respectively. For derivation of the WMR dynamics an extended coordinate set, $q = [x_b \ y_b \ \phi \ \theta_R \ \theta_L]^T$ is used. The dynamic equation of motion for the wheeled mobile robot (WMR)

with nonholonomic constraints can be obtained by the standard constrained Euler-Lagrangian formulation as:

$$\mathbf{M}(q)\ddot{q} + \mathbf{C}(q, \dot{q})\dot{q} + \mathbf{R}(q, \dot{q})\dot{q} = \mathbf{E}\tau - \mathbf{A}(q)^T \lambda \quad (17)$$

$$\mathbf{R} = \begin{bmatrix} 0 & 0 & 0 & 0 & 0 \\ 0 & 0 & 0 & 0 & 0 \\ 0 & 0 & 0 & 0 & 0 \\ 0 & 0 & 0 & c_{vR} & 0 \\ 0 & 0 & 0 & 0 & c_{vL} \end{bmatrix} \quad \mathbf{E} = \begin{bmatrix} 0 & 0 \\ 0 & 0 \\ 0 & 0 \\ 1 & 0 \\ 0 & 1 \end{bmatrix} \quad \mathbf{C} = \begin{bmatrix} 0 & 0 & 2a_1dc_\phi\dot{\phi} & 0 & 0 \\ 0 & 0 & 2a_1ds_\phi\dot{\phi} & 0 & 0 \\ 0 & 0 & 0 & 0 & 0 \\ 0 & 0 & 0 & 0 & 0 \\ 0 & 0 & 0 & 0 & 0 \end{bmatrix}$$

$$\mathbf{M} = \begin{bmatrix} a_2 & 0 & 2a_1ds_\phi & 0 & 0 \\ 0 & a_2 & -2a_1dc_\phi & 0 & 0 \\ 2a_1ds_\phi & -2a_1dc_\phi & a_3 & 0 & 0 \\ 0 & 0 & 0 & a_4 & 0 \\ 0 & 0 & 0 & 0 & a_4 \end{bmatrix} \quad \begin{aligned} a_1 &= m_w \\ a_3 &= I_b + 2m_w(d^2 + b^2) \\ a_2 &= m_b + 2m_w \\ a_4 &= I_w \end{aligned}$$

$$\mathbf{A} = \begin{bmatrix} -\sin\phi & \cos\phi & -d & 0 & 0 \\ \cos\phi & \sin\phi & b & -r & 0 \\ \cos\phi & \sin\phi & -b & 0 & -r \end{bmatrix}$$

where $\mathbf{M}(q)$ is the mass matrix, $\mathbf{C}(q, \dot{q})$ contains the Coriolis and centerfugal terms, $\mathbf{R}(q, \dot{q})$ is the friction matrix, $\mathbf{A}(q)^T$ is the constraint matrix, \mathbf{E} is the map from the actuation space to extended coordinate space and λ are the constraint forces maintaining the WMR holonomic and non-holonomic constraints. The constrained Euler-Lagrangian dynamics are projected into the feasible motion subspace as:

$$\mathbf{H}(q)\dot{v} + \mathbf{V}(q, \dot{q})v + \mathbf{D}(\dot{q})v = \mathbf{N}\tau \quad (18)$$

$$\begin{aligned} \mathbf{H}(q) &= \mathbf{S}^T \mathbf{M}(q) \mathbf{S} & \mathbf{D}(q) &= \mathbf{S}^T \mathbf{R}(q) \mathbf{S} \\ \mathbf{N} &= \mathbf{S}^T \mathbf{E} = \mathbf{I} & \dot{v} &= [\dot{\theta}_R, \dot{\theta}_L]^T \\ \mathbf{V}(q, \dot{q}) &= \mathbf{S}^T \mathbf{M}(q) \dot{\mathbf{S}} + \mathbf{S}^T \mathbf{C}(q, \dot{q}) \mathbf{S} \end{aligned}$$

3.2 Decoupling Matrix

This restricts the number of independent output equations to two. For teleoperation control, the Cartesian position $(x = [x_e, y_e]^T)$ of the look ahead point of the WMR was chosen as system outputs, giving the following input-output relationship between q and x :

$$x = h(q) = \begin{bmatrix} x_b + L_a c_\phi \\ y_b + L_a s_\phi \end{bmatrix} \quad (19)$$

A decoupling matrix can be formed to map the set of independent joint velocities to the desired output velocities. The decoupling matrix is 2 by 2 and must be full rank:

$$\Phi(q) = \mathbf{J}_h(q) \mathbf{S}(q)$$

$$= \begin{bmatrix} 1 & 0 & -L_a s \phi & 0 & 0 \\ 0 & 1 & L_a c \phi & 0 & 0 \end{bmatrix} \begin{bmatrix} c[b \cos \phi - d \sin \phi] & c[b \cos \phi + d \sin \phi] \\ c[b \sin \phi + d \cos \phi] & c[b \sin \phi - d \cos \phi] \\ c & -c \\ 1 & 0 \\ 0 & 1 \end{bmatrix} \quad (20)$$

$$= c \begin{bmatrix} b \cos \phi - (d + L_a) \sin \phi & b \cos \phi + (d + L_a) \sin \phi \\ b \sin \phi + (d + L_a) \cos \phi & b \sin \phi - (d + L_a) \cos \phi \end{bmatrix}$$

where $c = \frac{r}{2b}$ and $\mathbf{J}_h(q)$ is the output Jacobian for the WMR look ahead point. The determinant of the decoupling matrix is singular when $L_a = -d$, restricting the position of the look ahead point from being located on the axis of rotation of the drive wheels.

3.3 Output Synchronization of a WMR

The Phantom Omni haptic device is modeled as a translational mass and the feasible dynamic formulation of the WMR is used:

$$\mathbf{M}(q)_m \ddot{x}_m = F_m \quad (21)$$

$$\mathbf{H}(q)_s \dot{v}_s + \mathbf{V}(q, \dot{q})_s v_s + \mathbf{D}(\dot{q})_s v_s = \tau_s$$

using the local state output, the following passive control law is applied to each system:

$$F_m = \mathbf{M}(q)_m \ddot{x}_m^r + \bar{F}_m \quad (22)$$

$$\tau_s = \mathbf{Y}(q, v_s^r, \dot{v}_s^r) p_s + \bar{\tau}_s$$

where

$$\dot{x}_i^r = -\lambda x_i \quad \forall i \in m, s \quad v_i^r = -\lambda \begin{bmatrix} \theta_R^i \\ \theta_L^i \end{bmatrix} \quad \forall i \in m, s$$

$$\ddot{x}_i^r = -\lambda \dot{x}_i \quad \forall i \in m, s \quad \dot{v}_i^r = -\lambda v_i \quad \forall i \in m, s$$

The decoupling matrix provides a mapping between the independent joints space (v) and Cartesian output space, x :

$$\dot{x} = \Phi(q)v \quad \text{and} \quad v = \Phi(q)^{-1} \dot{x}$$

Using the decoupling mapping, a Cartesian synchronization control law can be found which passively couples the system irrespective of the local generalized coordinates [14].

$$\bar{F}_m = \mathbf{K} [r_s(t-T) - r_m] \quad (23)$$

$$\bar{\tau}_s = \mathbf{K} \Phi(q)_s^{-1} [r_m(t-T) - r_s(t)]$$

where,

$$r_m = \dot{x}_m - \dot{x}_m^r = \dot{x}_m + \lambda x_m, \quad r_s = \dot{x}_s - \dot{x}_s^r = \dot{x}_s + \lambda x_s$$

4 HARDWARE IN THE LOOP SIMULATION FRAMEWORK

This section discusses the real time framework used for coupling the master and slave devices in a hardware-in-the-loop (HIL) simulation framework. As seen in Figure 3, the master device is a physical Phantom Omni whereas the slave device here is a simulated WMR rolling on flat ground.



FIGURE 3: REAL TIME IMPLEMENTATION FRAMEWORK.

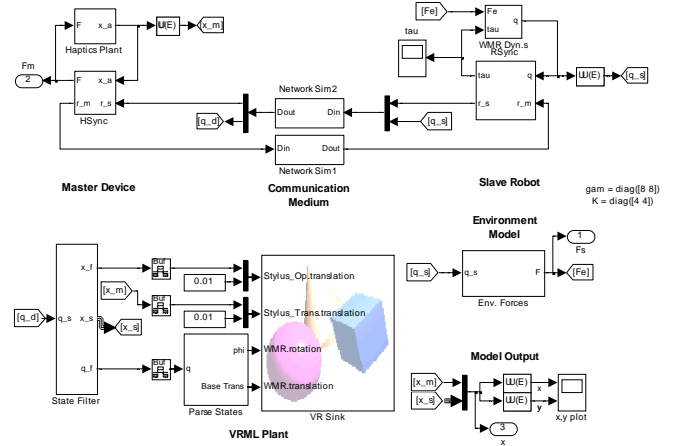


FIGURE 4: THE WMR SIMULATION.

This HIL simulated teleoperation control was run on a single laptop computer using a Virtual Network Interface between master and slave systems. The key subsystems include the haptic and slave control blocks, a stochastic network simulator and a three dimensional visual output. The master system position is indicated by a small solid sphere. The human user is free to move the sphere anywhere within the workspace of the haptic device. Separate VRML scenes were created containing a scaled three dimensional model of the WMR.

The WMR output synchronization scheme and dynamics were used to simulate the slave manipulator. The kinematic and dynamic parameters for the haptic device and simulated WMR are summarized in Table 1.

TABLE 1: WHEELED MOBILE ROBOT PARAMETERS.

Parameter	Value	Parameter	Value
m_w	0.1 kg	d	0.146 m
m_b	17.25 kg	b	0.168 m
I_w	2e-4 kg · m ²	c_R	0.1 kg · m ² /s
I_B	17.25 kg · m ²	c_L	0.1 kg · m ² /s
r	0.051 m	M	diag(1e-3, 1e-3) kg

The haptic output subsystem contained a new model reflecting the WMR system. A virtual wall is added to provide a virtual surface for the WMR to interact with.

TABLE 2: BOX HAPTIC PARAMETERS.

Parameter	Value	Parameter	Value
Box Size [w, h, d]	[1, 1, 0.5] m	Box Center Location	[0.9 0 0] m
Stiffness	100,000 N/m	Coulomb Friction	1.0
Damping Factor	40	Velocity threshold for coulomb friction	20

5 RESULTS

Table 3 highlights the two cases selected to test the proposed teleoperation control scheme.

TABLE 3: A SUMMARY OF TEST CASES

Case	Delay Type	Comm. Reliability
I	Constant 0.001 sec	0% Random Loss
II	Normal distribution mean = 0.4 sec, std = 0.12 sec	55% Random Loss

The delay type and communication reliability represent the network conditions for data traveling in one direction over the network (from master to slave or visa versa). Total delay for a single loop is two times the value presented here. In this section, the teleoperation abilities for a wheeled mobile robot are explored to demonstrate the algorithms robustness to packet loss and constant and variable time delays. In both cases, the haptic device is commanded to follow the following time varying Cartesian trajectories:

$$\begin{aligned} x &= 3e - 4t^4 - 8.2e - 3t^3 + 0.052t^2 - 0.0351t + 9.4e - 3 \\ y &= 0 \end{aligned} \quad (24)$$

5.1 Case I: Idealized Perfect Network

For the first case study, the WMR is teleoperated with a lossless communication channel and very low time delay. This test is meant to serve as a base-reference to verify functioning of bilateral teleoperation of the differentially driven wheel mobile robot in the absence of any delays. An initial position offset ($x = 0$ and $y = -0.05m$) is introduced to verify that the proposed algorithm can converge to the desired position in free space. The following control gains were used during a 15 seconds simulation.

$$\lambda = \begin{bmatrix} 5 & 0 \\ 0 & 5 \end{bmatrix}, \quad \mathbf{K} = \begin{bmatrix} 3 & 0 \\ 0 & 3 \end{bmatrix}$$

Figure 5 contains the Cartesian position and force tracking results for Case I. In the absence of time delay, the master and

slave systems have very good tracking results. Despite the initial $y = -0.05m$ offset at the start of the simulation, the WMR slave robot successfully converged to the desired master trajectory. A spike in the “y” slave trajectory appears while the WMR is driving backwards from the wall, due to the instability of the look ahead controller when driving backwards (as pointed out in [19]). This instability causes the WMR quickly turn around and resume driving along the trajectory in the forward direction.

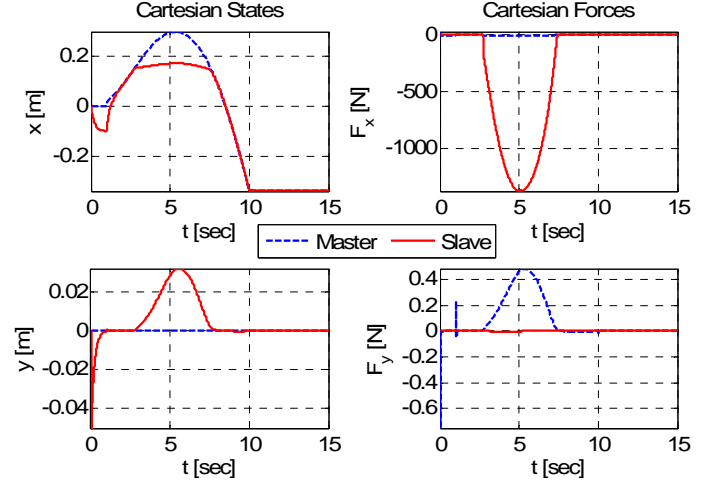


FIGURE 5: CASE I - TELEOPERATION OF A WMR WITHOUT TIME DELAY AND PACKET LOSS.

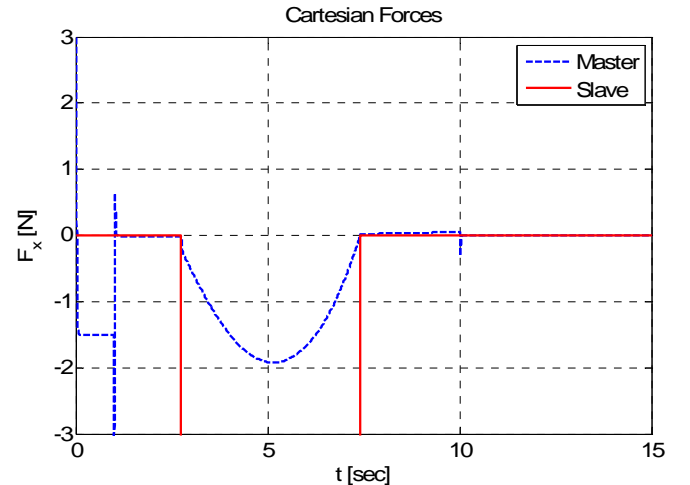


FIGURE 6: CLOSEUP VIEW OF THE FORCE PROFILE SHOWN IN TOP RIGHT OF FIGURE 5.

Large forces, such as those shown in Fig. 5 (top right), ($F_x = -1500N$ at $t = 5$ sec) can occur within simulations as a result of contact with the environment without limits being placed on actuation capacity and by strict enforcement of the no slip condition. Similar magnitude of forces can also arise for real-life tests when contacting with hard objects. Within this framework, however these large forces are not reflected back to the master device/user. Doing so would have the potential of damaging the device, hurting the user, or potentially destabilizing the bilateral teleoperation. Instead a scaled force proportional to the slave

forces is reflected back, shown in greater detail in Fig. 6, which allows for correction of the tracking error. The Cartesian forces in the y direction (Fig. 5 bottom right) are extremely small and are byproducts of the friction model of the block. Figure 5 also contains the plots of master and slave force profiles.

5.2 Case II: Lossy, Delayed Network

For the second scenario, the WMR was teleoperated over an extremely lossy and delayed network environment.

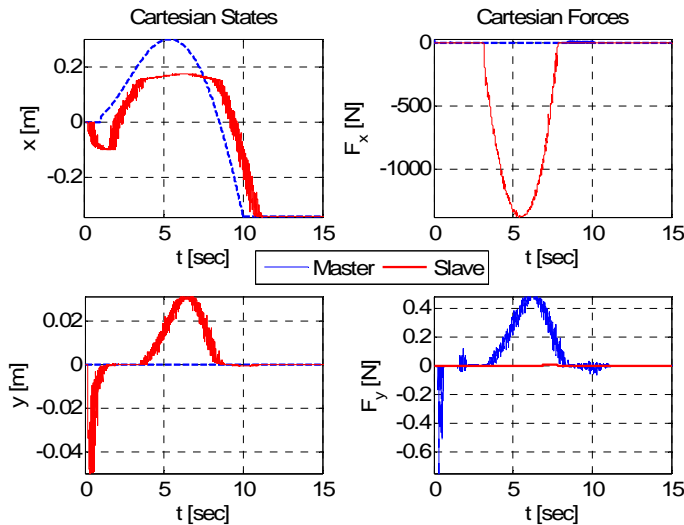


FIGURE 7: CASE II - TELEOPERATION UNDER VARIABLE TIME DELAY (MEAN = 0.4 SEC, STD = 0.12 SEC) AND 55% PACKET LOSS.

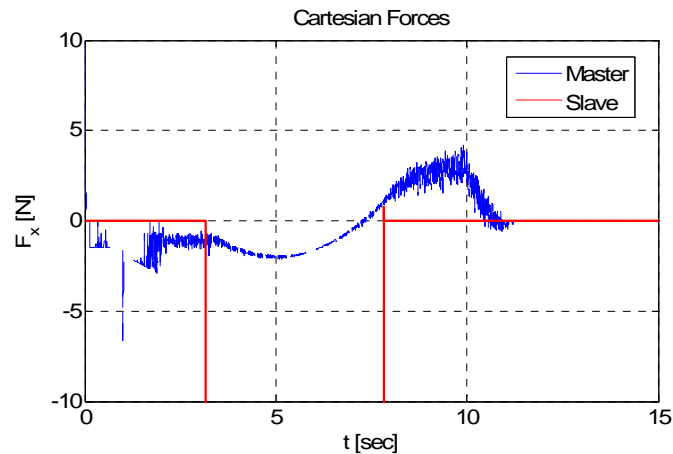


FIGURE 8: CLOSEUP VIEW OF THE FORCE PROFILE SHOWN IN TOP RIGHT OF FIGURE 7.

A variable network delay modeled by a normal distribution latency with an average value of 0.4 seconds and standard deviation of 0.12 seconds. This delay was mimicked in both receiving and transmitting directions. Data packets were randomly lost at a rate of 55% with a buffer maintaining the most recent packet values. The scenario suggests that even in the most volatile of network conditions, the master and slave systems will still remain stable. The haptic device was commanded in the predefined trajectory with an initial position of

$x = 0$ and $y = -0.05m$ and simulated for 15 seconds. The gains λ and \mathbf{K} were the same as Case I. The simulated position and force results for Case II are presented in Figure 7. The position results have an offset in tracking performance due to the large variable delay and packet loss between master and slave. Large forces are once again experienced around $t = 5$ sec, when contact is made with the virtual object (Fig. 7 (top right), which is shown in greater detail in Fig. 8). Despite an initial offset, the master and slave did states remained bounded and, in the case of the y Cartesian direction, tracked well. While the position and force results are noisy, the controller did not destabilize despite the extreme network conditions.

6 DISCUSSION

A passivity based synchronization framework was introduced with the stability of the controller analyzed. A hybrid Cartesian bilateral teleoperation control scheme was developed to couple a Phantom Omni system and simulated wheeled mobile robot. The framework contained several passive elements including an adaptive controller used to estimate dynamic parameters in real time for improved tracking results. This hybrid controller has the ability to be turned on and off at the press of a button.

A set of HIL simulations were performed to test the capabilities of the synchronization controller. The controller was tested with both ideal and delayed and lossy network conditions to validate both free space and hard contact scenarios. Despite initial position offsets between master and slave systems, position synchronization was achieved. The framework also remained stable when the slave system came in contact with a virtual rigid obstacle despite volatile network conditions. Future work involves experimental testing (see Fig. 9) is currently underway.

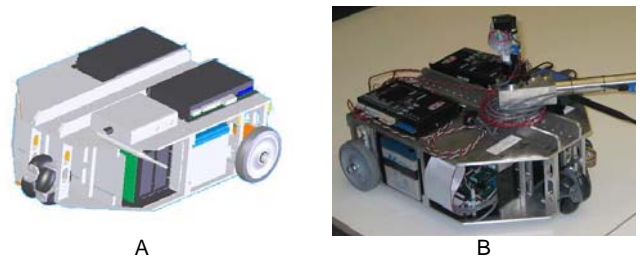


FIGURE 9: (A) THE PROTOTYPE WHEEL MOBILE ROBOT; (B) ACTUAL WHEEL MOBILE ROBOT.

REFERENCES

- [1] N. Chopra, M. W. Spong, and R. Lozano, "Synchronization of bilateral teleoperators with time delay," *Automatica*, vol. 44, p. 6, July 19 2007.
- [2] P. F. Hokayem and M. W. Spong, "Bilateral teleoperation: An historical survey," *Automatica*, vol. 42, p. 22, April 12 2006.
- [3] R. J. Anderson and M. W. Spong, "Bilateral Control of Teleoperators with Time Delay," *Transactions on Automatic Control*, vol. 34, p. 8, May 1989.

- [4] G. Niemeyer and J.-J. E. Slotine, "Stable Adaptive Teleoperation," *Journal of Oceanic Engineering*, vol. 16, p. 11, January 1991.
- [5] N. Chopra and M. W. Spong, "Adaptive Coordination Control of Bilateral Teleoperators with Time Delay," in *Conference on Decision and Control*, IEEE, Ed. Atlantis, Paradise Island, Bahamas, 2004, pp. 4540 - 4547.
- [6] N. Chopra, M. W. Spong, R. Ortega, and N. E. Barabanov, "On Tracking Performance in Bilateral Teleoperation," *Transactions on Robotics*, vol. 22, p. 6, August 2006.
- [7] G. Niemeyer and J.-J. E. Slotine, "Towards Force-Reflecting Teleoperation Over the Internet," in *International Conference on Robotics and Automation*, Leuven, Belgium, 1998, pp. 1909 - 1916.
- [8] J.-H. Ryu, D.-S. Kwon, and B. Hannaford, "Stable Teleoperation with Time-Domain Passivity Control," in *IEEE Transactions on Robotics and Automation*. vol. 20, 2004, pp. 365-373.
- [9] Y. Ye and P. X. Liu, "Improving Force Feedback Fidelity in Wave-Variable Based Teleoperation," in *IEEE International Conference on Robotics and Automation* Pasadena, CA, 2008, pp. 194 - 199.
- [10] M. W. Spong and N. Chopra, "Synchronization of networked Lagrangian Systems," *Lagrangian and Hamiltonian methods for nonlinear control*, p. 12, 2007.
- [11] J.-J. E. Slotine and W. Li, *Applied Nonlinear Control*, 1 ed. Upper Saddle River: Prentice Hall International Inc., 1991.
- [12] M. W. Spong, S. Hutchinson, and M. Vidyasagar, *Robot Modeling and Control*: John Wiley & Sons, Inc., 2006.
- [13] D. Lee, O. Martinez-Palafox, and M. W. Spong, "Bilateral Teleoperation of a Wheeled Mobile Robot over Delayed Communication Network," in *International Conference on Robotics and Automation*, Orlando, Florida, 2006, p. 3298.
- [14] P. Miller, "Output synchronization for teleoperation of robot manipulators," in *Mechanical and Aerospace Engineering*. vol. M.S. Buffalo: State University of New York at Buffalo, 2009, p. 104.
- [15] N. Chopra, "Output Synchronization of Networked Passive Systems." vol. Ph. D Urbana: University of Illinois at Urbana-Champaign, 2006, p. 155.
- [16] P. A. Ioannou and J. Sun, *Robust Adaptive Control*: Prentice-Hall, 1996.
- [17] X. Yun, V. Kumar, and N. Sarkar, "Control of multiple arms with rolling constraints," in *International Conference on Robotics and Automation*, IEEE, Ed. Nice, France, 1992, pp. 2193 - 2198.
- [18] N. Sarkar, X. Yun, and V. Kumar, "Control of Mechanical Systems with Rolling Constraints: Application to Dynamic Control of Mobile Robots," University at Pennsylvania, Philadelphia, PA.
- [19] X. Yun and Y. Yamamoto, "Internal Dynamics of a Wheeled Mobile Robot," *Journal of Robotic Systems*, vol. 14, p. 12, 1997.